NACA

RESEARCH MEMORANDUM

EFFECT OF AN ADJUSTABLE SUPERSONIC INLET ON THE PERFORMANCE UP TO MACH NUMBER 2.0 OF A J34 TURBOJET ENGINE

By Andrew Beke, Gerald Englert, and Milton Beheim

Lewis Flight Propulsion Laboratory
Cleveland, Ohio

NATIONAL ADVISORY COMMITTEE
FOR AERONAUTICS

WASHINGTON

January 4, 1956

NACA RM E55I27

NATIONAL ADVISORY COMMITTEE FOR AERONAUTICS

RESEARCH MEMORANDUM

EFFECT OF AN ADJUSTABLE SUPERSONIC INLET ON THE PERFORMANCE UP TO MACH NUMBER 2.0 OF A J34 TURBOJET ENGINE

By Andrew Beke, Gerald Englert, and Milton Beheim

SUMMARY

A J34 turbojet engine was investigated at Mach numbers of 0.12, 1.6, 1.8, and 2.0 to determine the effect of supersonic inlet operation on engine performance. A combination translating spike and variable bypass inlet was used. With the exception of ideal jet thrust, the use of generalized engine parameters correlated the engine data satisfactorily when the exit nozzle was choked. In particular, large total-pressure distortions did not affect the engine compressor efficiency.

During inlet pulsing, the engine operated with compressor-inlet total-pressure variations as large as 18 percent of the local average and at frequencies of 17 ±2 cycles per second. Total-pressure amplitudes propagated through the engine and at the exit nozzle were as much as 5 percent of the local total pressure. Fluctuation of the nozzle total pressure caused ideal-gross-thrust changes up to 12 percent.

INTRODUCTION

Turbojet engine performance is generally obtained by simulating at the compressor inlet the one-dimensional steady-state conditions to be encountered in flight. This technique does not necessarily simulate conditions encountered in flight which may limit the engine thrust output. For example, inlet pulsing and flow distortion which may be present with oblique-shock-type supersonic air inlets may seriously restrict the application of the turbojet engine in the supersonic speed range.

A general investigation was undertaken in the Lewis 8- by 6-foot supersonic wind tunnel to determine the performance of a typical turbojet engine at supersonic speeds. A J34 engine was operated at Mach numbers from 1.5 to 2.0 and zero angle of attack behind an axially symmetrical, variable-geometry spike inlet. The inlet spike could be translated over a range of tip projections and as much as 20 percent of the inlet flow could be bled out through bypass slots in the diffuser. The effect of

the engine on the inlet performance is reported in references 1 and 2. Reported herein is the effect of the inlet and its operating conditions on the performance of the engine.

SYMBOLS

The following symbols are used in this report:

A_f	frontal area of compressor rotor, 1.98 sq ft
A_5^*	nozzle exit area, 1.29 sq ft
F_i	ideal gross thrust of an exit nozzle reexpanding to free-stream static pressure
f	frequency, cps
M	Mach number
N	engine rotational speed, rpm
N^*	rated engine speed, 12,500 rpm
$\frac{N}{N^*\sqrt{\theta}}$	corrected engine speed ratio
P	total pressure
p	static pressure
r	radial distance from hub at compressor face
T	total temperature
w_a	air flow rate
w_f	fuel flow rate
$\frac{w_a\sqrt{\theta}}{\delta A_f}$	corrected air flow rate per unit area
$\frac{w_f}{\delta\sqrt{\theta}}$	corrected fuel flow rate
γ	ratio of specific heats

δ ratio of absolute total pressure to NACA standard sea-level absolute pressure

η_c compressor adiabatic efficiency

θ ratio of absolute total temperature to NACA standard sea-level absolute temperature

θ_l angle between spike axis and line joining cone apex and cowl lip

Subscripts:

av average

l local (pressure)

max maximum

min minimum

w windmilling

0 undisturbed free stream

3 compressor inlet, station 62.5

5 nozzle, station 179

APPARATUS AND PROCEDURE

The nacelle installation of the J34 turbojet engine in the 8- by 6-foot supersonic wind tunnel is shown in figure 1. This same configuration was used in the investigations of references 1 and 2. Briefly, the engine was a standard production model with an 11-stage axial-flow compressor, a two-stage turbine, and a fixed-area convergent jet exhaust nozzle. Rated engine air flow is 58 pounds per second and the rated thrust is 3000 pounds at maximum rated speed (12,500 rpm) and standard static sea-level conditions. Other details concerning engine installation and operation are reported in references 1 and 2.

The air induction system for the engine (fig. 1) consisted of a translating 25°-half-angle conical-spike nose inlet. The spike could be translated longitudinally, and four spike positions (θ_l = 51°, 46°, 42.6°, and 38.4°) were investigated. These spike-position-parameter angles correspond to inlet operation with the oblique shock at the cowl lip at Mach

numbers of 1.6, 1.8, 2.0, and 2.4, respectively. Bypass air bleed slots were located in the subsonic diffuser outer wall (station 40).[1] The bypass door (fig. 1) was used either in the closed or fully opened position. Details of the variation in inlet design and diffuser area for the various spike positions are reported in references 1 and 2.

Total-pressure and total-temperature instrumentation was located at various stations as shown in figure 1. Engine gas flow was computed from the exit nozzle total temperatures and pressures and the throat area, while engine fuel flow was recorded from standard flow metering devices. The maximum thrust potential of the engine (thrust of an ideal reexpanding exhaust nozzle) was computed from tail-pipe total temperatures and pressures. All the generalized engine data were referred to the compressor-inlet total temperature and pressure at station 62.5.

Unsteady-flow pressure data (engine operation with inlet pulsing) were recorded at several nacelle longitudinal stations in order to detect and trace pulse propagation through the inlet, engine, and tail pipe. Dynamic total-pressure pickups were located about an inch from the outer wall in the diffuser at stations 10 and 62.5, at the compressor fifth and seventh stages (stations 85 and 92), at the compressor outlet (station 102), and in the tail pipe at station 179. Pulse amplitudes were evaluated from static calibration of the dynamic probes and oscillograph traces obtained at each measuring station in the diffuser, while average total pressures in the engine and tail pipe were obtained from steady-state instrumentation. Unsteady-inlet-flow data were also obtained with the engine removed. Diffuser operation was then controlled with a choked exit plug (see ref. 2).

RESULTS AND DISCUSSION

Steady-State Inlet Operation

Diffuser performance in terms of total-pressure recovery and corrected engine air flow are presented in figure 2. Typical diffuser-exit total-pressure distortions for a constant value of engine corrected air flow are shown in figure 3. Large variations in compressor-inlet flow conditions were imposed on the engine by the supersonic inlet. In some cases the total-pressure distortions were as great as 13 percent of the average local total pressure. For any given corrected air flow (fig. 2), significantly large variations in diffuser total-pressure recovery occurred as spike position was varied. However, because several of these spike positions were for off-design inlet conditions, an engine operating behind a supersonic inlet in actual flight probably would not be subjected to the large distortions indicated herein.

[1]Station numbers denote distance in inches from cowl lip.

Compressor efficiency for the various free-stream Mach numbers and spike positions investigated is presented in figure 4. When the engine remained on the same operating line (exit nozzle choked), the compressor efficiency appeared to be unaffected by changes in supersonic free-stream Mach number (fig. 4(a)). However, when the engine operated in a subsonic free stream, a difference in compressor efficiency occurred because of unchoking of the exit nozzle, and a consequent shift in the equilibrium operating line was noted. Within the accuracy of the data in figure 4(b), no significant effect of spike position on compressor efficiency is observed.

Inasmuch as changes in flight speed and spike position caused significant changes in flow distortions at the compressor face (fig. 3) but did not affect compressor efficiency when the nozzle was choked (fig. 4), it follows that large total-pressure distortions accompanying these flight-speed and spike-position variations were not of sufficient magnitude to affect the engine compressor efficiency.

Generalized engine characteristics in terms of corrected engine variables are presented in figure 5. Corrected air flow, fuel flow, and engine pressure and temperature ratios in figures 5(a), (b), and (c) are presented for two spike positions only, because the use of the generalized engine parameters correlated all these data satisfactorily when the nozzle was choked. Differences between subsonic and supersonic characteristics are due to unchoking of the exit nozzle. Thrust data in figures 5(d) and (e), calculated from measured engine pressure ratio for a completely expanded nozzle, show significant changes with free-stream Mach numbers and small variations with spike position. The reason ideal gross thrust did not generalize may be explained from the relation expressed in equation (1). The equation for ideal jet thrust is written in terms of engine pressure ratio (P_5/P_3) and inlet pressure recovery (P_3/P_0), as follows:

$$\frac{F_i}{\delta_3} = 2116 \left[\frac{\gamma \sqrt{\frac{2}{\gamma - 1}}}{\left(\frac{\gamma + 1}{2} \right)^{\frac{\gamma+1}{2(\gamma-1)}}} \right]_5 A_5^* \left(\frac{p}{P} \right)_0 \frac{1}{\left(\frac{P_3}{P_0} \right)} \sqrt{\left(\frac{P_5}{P_3} \frac{P_3}{P_0} \frac{P_0}{p_0} \right)^2 - \left(\frac{P_5}{P_3} \frac{P_3}{P_0} \frac{P_0}{p_0} \right)^{\frac{\gamma_5+1}{\gamma_5}}} \qquad (1)$$

Since the engine pressure ratio generalized when the nozzle was choked (fig. 5(c)), it is apparent from equation (1) that at a given engine corrected speed ratio the thrust is reduced to a function of both flight speed and inlet flow pressure recovery. Figures 5(d) and (e) reflect these effects. Nearly the same variation of thrust with spike position as shown in figure 5(e) was obtained at other free-stream Mach numbers.

Corrected engine windmilling speed ratios (zero fuel flow, fig. 5(b)), are plotted in figure 6. Successful windmill engine starts were performed at the free-stream Mach number and engine speeds indicated. Similar data were obtained for other inlet spike positions.

Pulsing Inlet Operation

Although large total-pressure fluctuations were encountered by the engine when it was operated with unsteady inlet flow (fig. 7(a)), it continued to perform satisfactorily. The magnitude of the fluctuation varied through the nacelle but generally was greatest in the compressor and least in the tail pipe. The frequency of pulsing remained between 15 and 17 cycles per second over the range of variables studied. In figure 7(b) the amplitude is referenced to the local average pressure. In general, the engine appeared to have exerted a damping influence on the amplitude ratio. With a compressor-inlet total-pressure oscillation as large as 18 percent of the local average ($M_0 = 2.0$, $\theta_l = 42.6^\circ$, bypass closed), the exit nozzle total pressure varied by about 5 percent. Additional data for pulse phenomenon at the diffuser discharge (station 62.5) are reported in reference 2.

As might be expected, pulse propagation through the system with engine removed (plug-exit model of ref. 2) was considerably different from that with the engine present. From figures 8(a) and (b), it may be seen that there was no consistent trend of either total-pressure amplitudes or ratios. In nearly all cases, the general trend indicated little reduction in pulse amplitude from inlet to exit, maximum variations of inlet and nozzle exit total pressure being about equal and ranging between 15 and 20 percent of average values. Pulsing frequencies were slightly lower than those with the engine installed and ranged between 8 and 14 cycles per second.

Representative pulse traces for each dynamic pickup station are shown in figure 9. Except for the inlet station (station 10), the characteristic pressures varied almost sinusoidally with time. Undoubtedly, the irregular wave shape at the inlet station (10) was caused by the movement of the terminal shock across the dynamic pickup.

Total-pressure oscillations in the exit nozzle are believed to have induced proportional variations in the jet thrust. Figure 10 shows the computed thrust changes due to the variations shown in figure 7 and for additional data ($\theta_l = 42^\circ$) where the exit nozzle total pressure varied about 10 percent. Approximate peak-thrust amplitudes, which represent absolute-thrust changes from 300 to 350 pounds, ranged between 8 and 12 percent of ideal gross thrust. Inasmuch as these thrust variations occur nearly simultaneously with the additive drag changes (or are related by a certain phase lag), the mean value of the net propulsive thrust of the system during unsteady inlet flow conditions may be seriously penalized.

SUMMARY OF RESULTS

An experimental investigation in the Lewis 8- by 6-foot supersonic wind tunnel of the J34 turbojet engine operating with an adjustable inlet up to a Mach number of 2.0 indicated the following results:

1. Use of the generalized engine parameters correlated the data satisfactorily when the exit nozzle was choked. Thrust did not correlate because of the variation of inlet total-pressure recovery and flight Mach number.

2. Compressor efficiency was unaffected by total-pressure distortions of 13 percent at the compressor inlet.

3. At a free-stream Mach number of 2.0, the engine was operated without failure in the region of inlet pulsing. Most severe conditions imposed were a compressor-inlet total-pressure maximum amplitude of 18 percent of the local average and a frequency of 17 ±2 cycles per second.

4. Although the engine may have exerted a damping influence during inlet pulsing, total-pressure amplitudes were propagated through the flow system, and, from a value of 22 percent of the local total pressure at the diffuser inlet, were reduced to a value of about 5 percent of the local total pressure at the exit nozzle.

5. Nozzle pulsating total pressures caused up to 12-percent changes in the calculated gross thrust.

Lewis Flight Propulsion Laboratory
National Advisory Committee for Aeronautics
Cleveland, Ohio, September 27, 1955

REFERENCES

1. Nettles, J. C., and Leissler, L. A.: Investigation of Adjustable Supersonic Inlet in Combination with J34 Engine up to Mach 2.0. NACA RM E54H11, 1954.

2. Beheim, Milton A., and Englert, Gerald W.: Effects of a J34 Turbojet Engine on Supersonic Diffuser Performance. NACA RM E55I21, 1955.

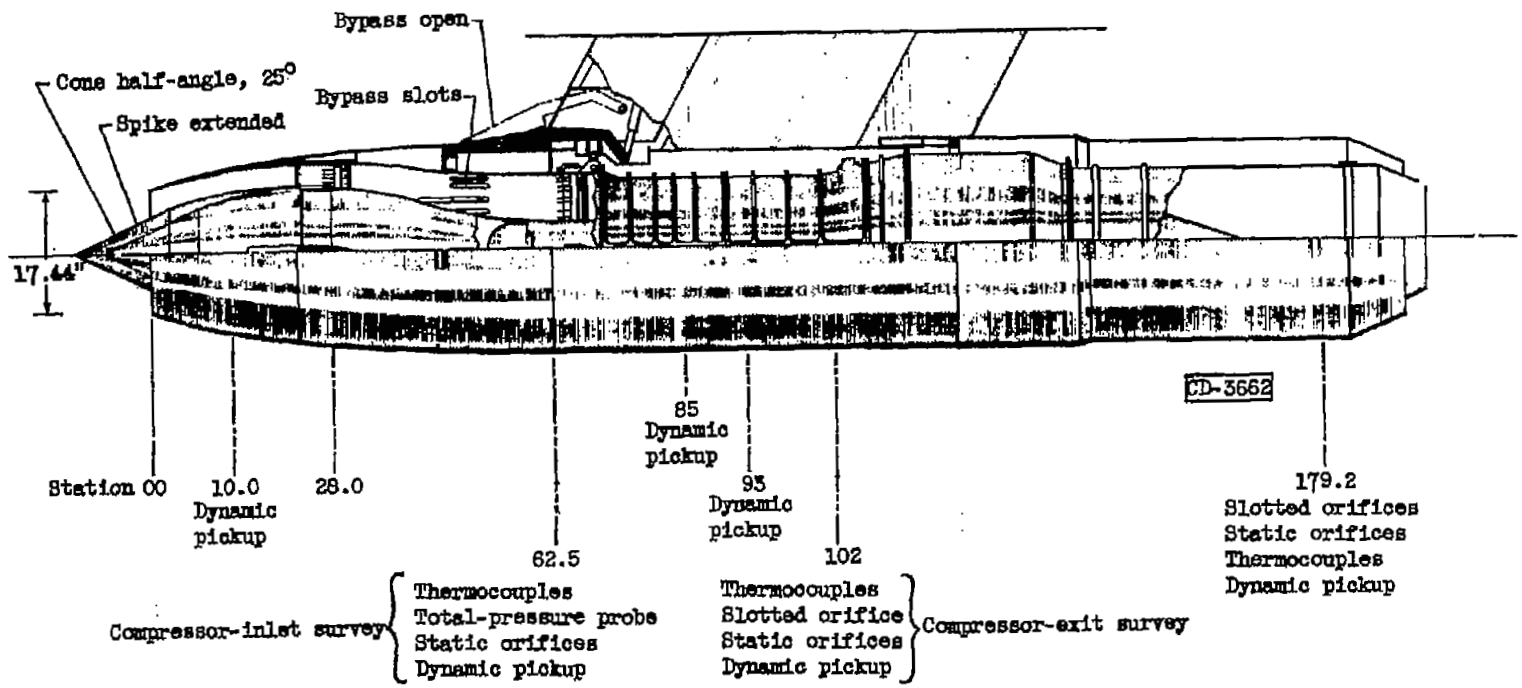

(a) Inlet-engine configuration.

Figure 1. - Nacelle installation of J34 turbojet engine.

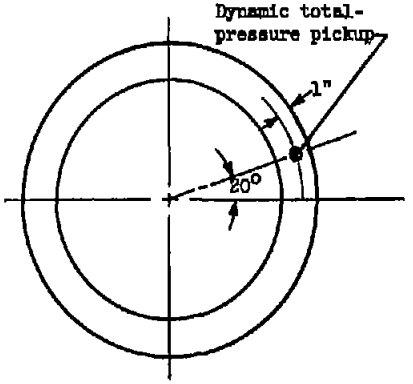

Inlet, station 10

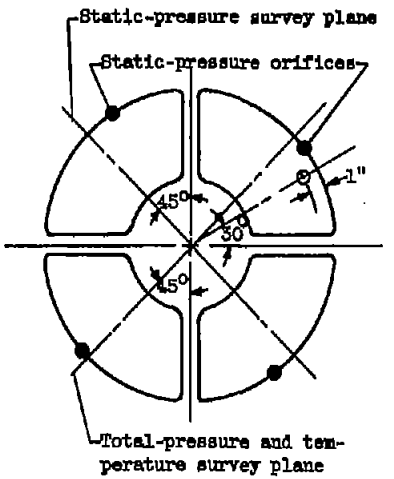

Compressor face, station 62.5

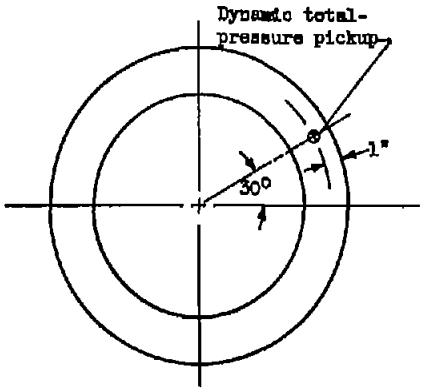

Compressor fifth stage, station 85

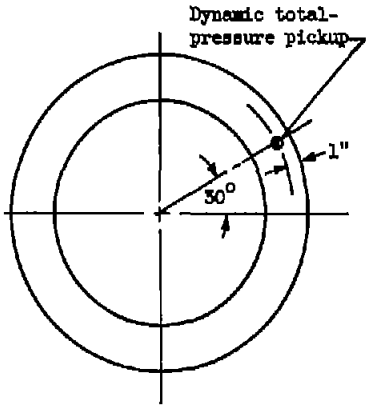

Compressor seventh stage, station 93

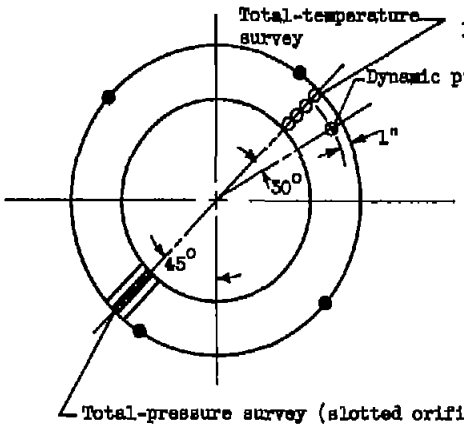

Compressor exit, station 102

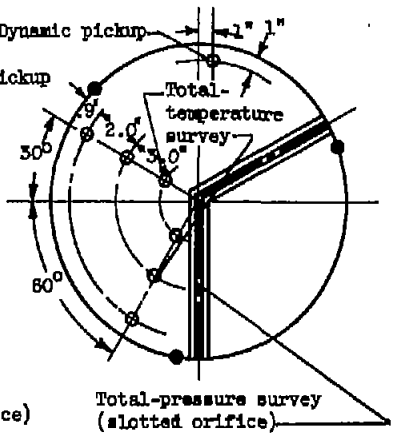

Nozzle entrance, station 179

(b) Details of instrumentation at various inlet-engine and nozzle stations.

Figure 1. - Concluded. Nacelle installation of J34 turbojet engine.

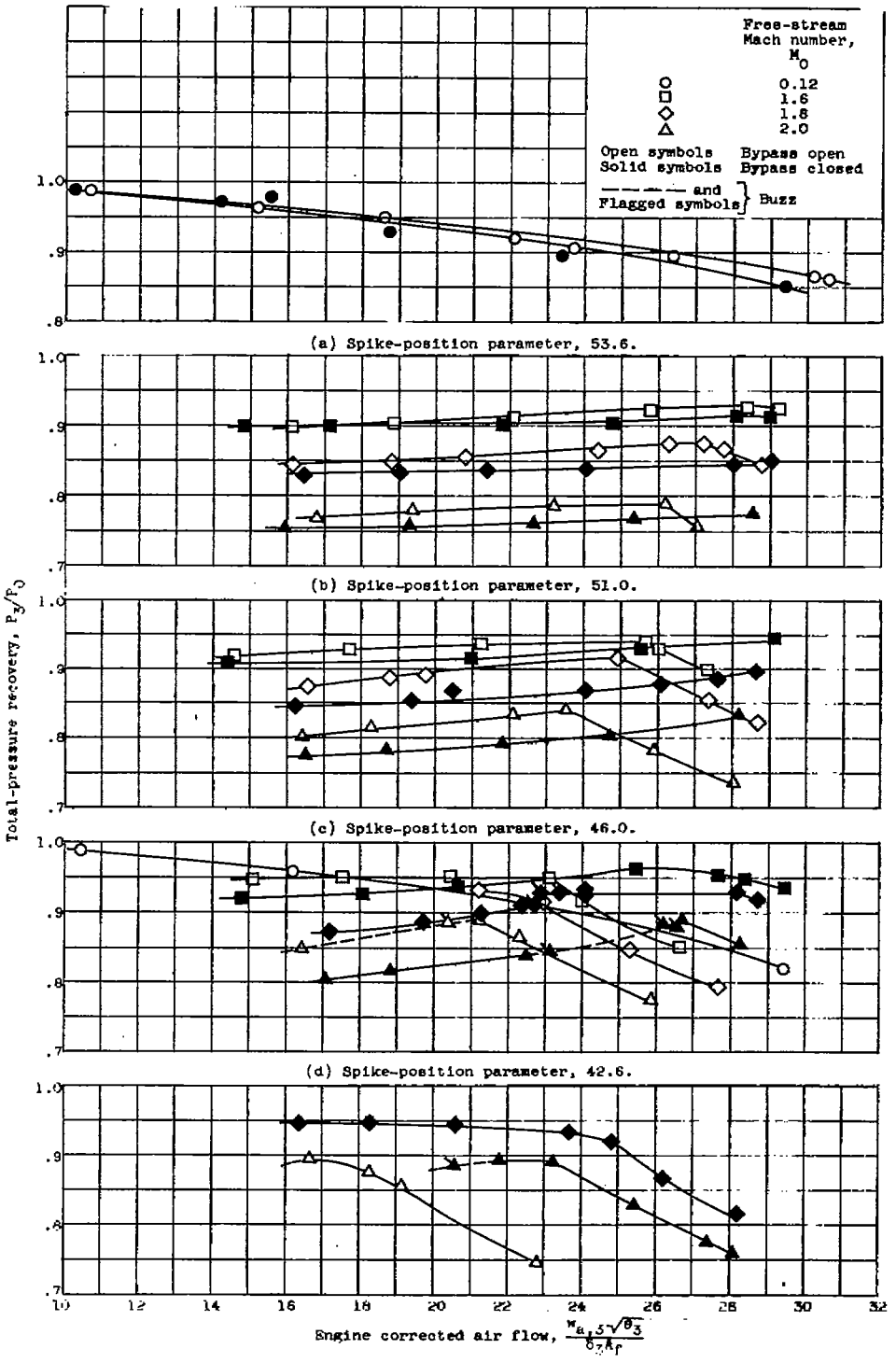

(a) Spike-position parameter, 53.6.

(b) Spike-position parameter, 51.0.

(c) Spike-position parameter, 46.0.

(d) Spike-position parameter, 42.6.

(e) Spike-position parameter, 38.4.

Figure 2. - Diffuser performance (ref. 2).

[redacted]

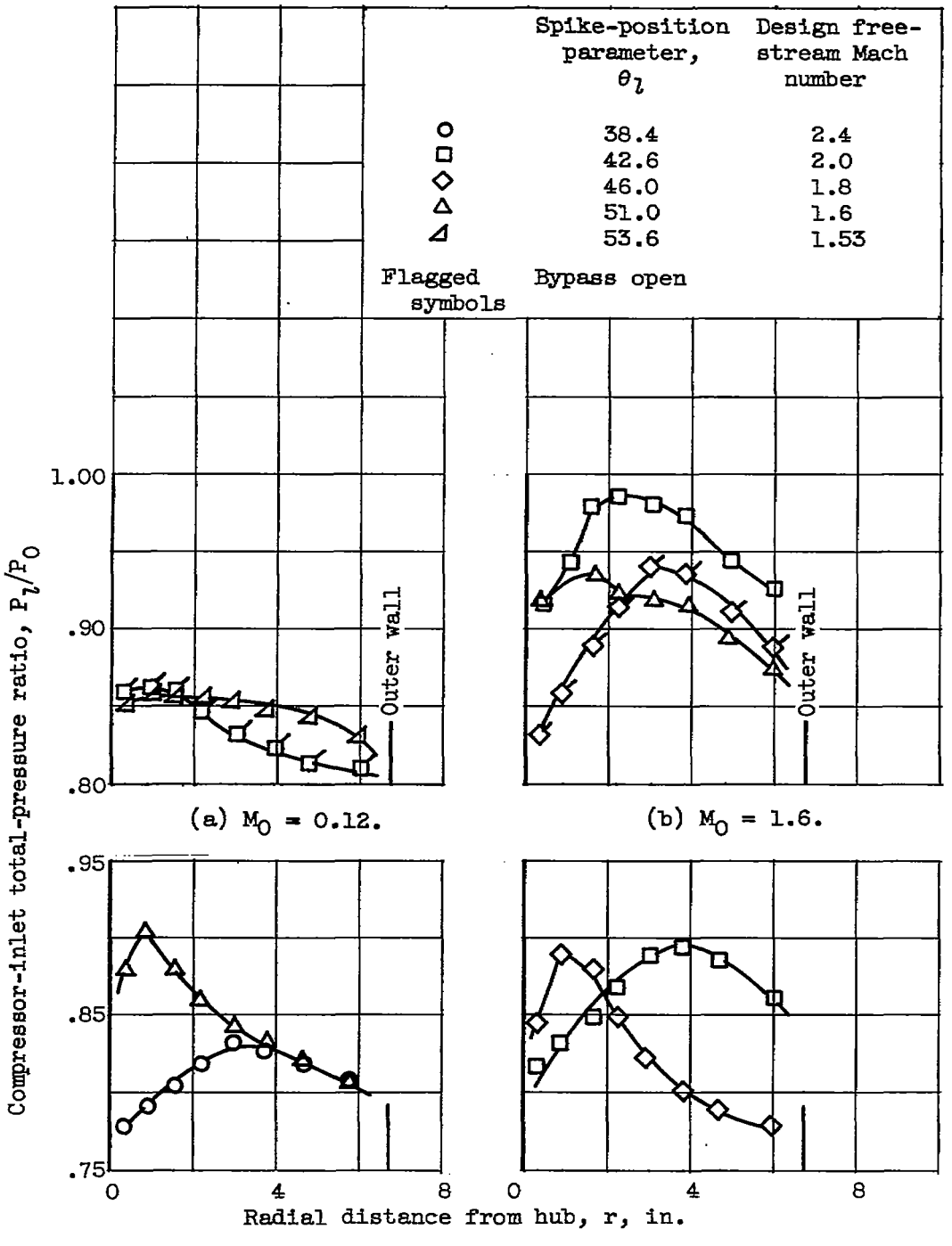

Figure 3. - Total-pressure profiles at compressor face, station 62.5. Corrected engine speed ratio, approximately 0.92.

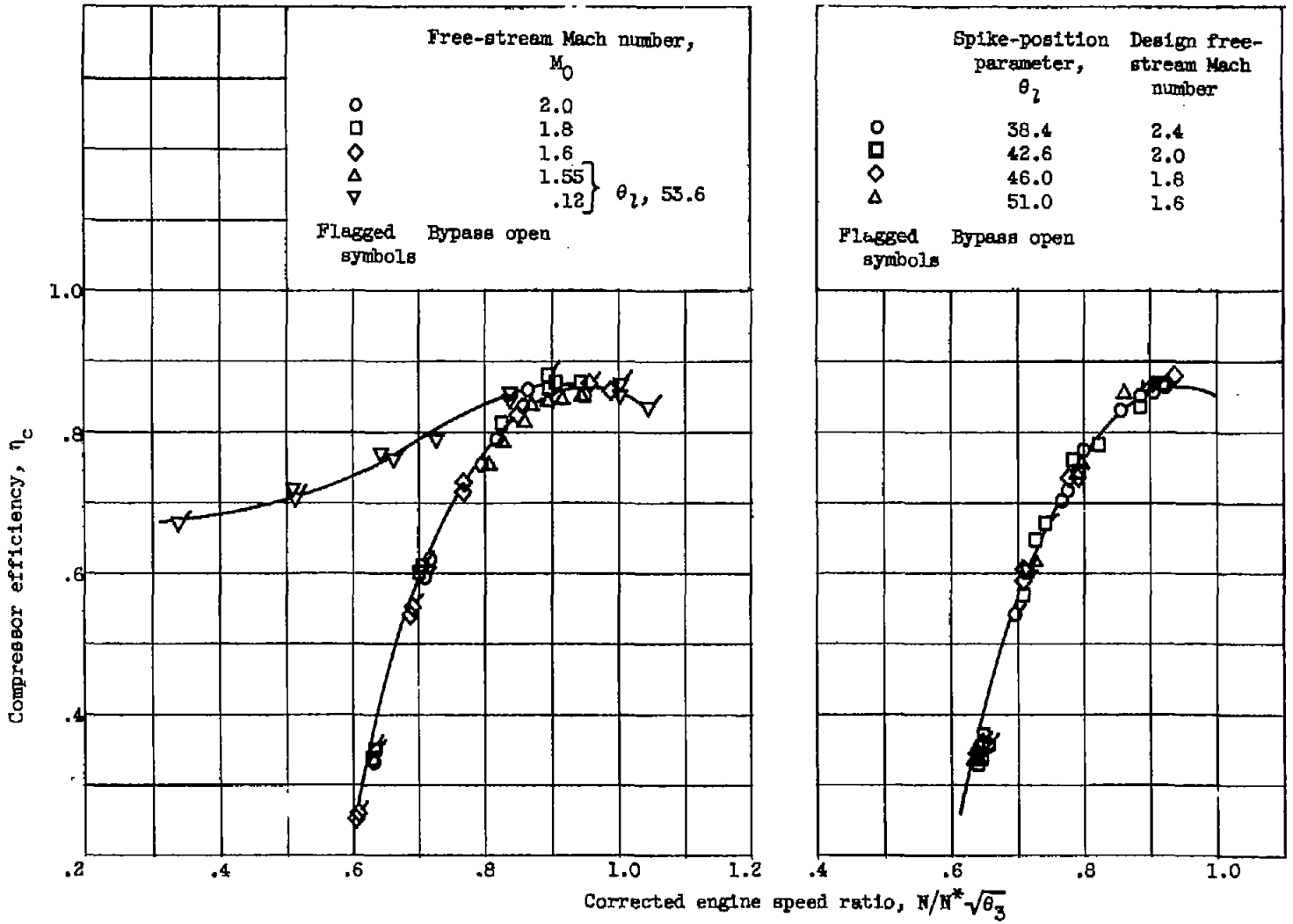

(a) Spike position parameter, θ_1, 51.0.

(b) Free-stream Mach number, M_0, 2.0.

Figure 4. - Variation of compressor efficiency with engine speed.

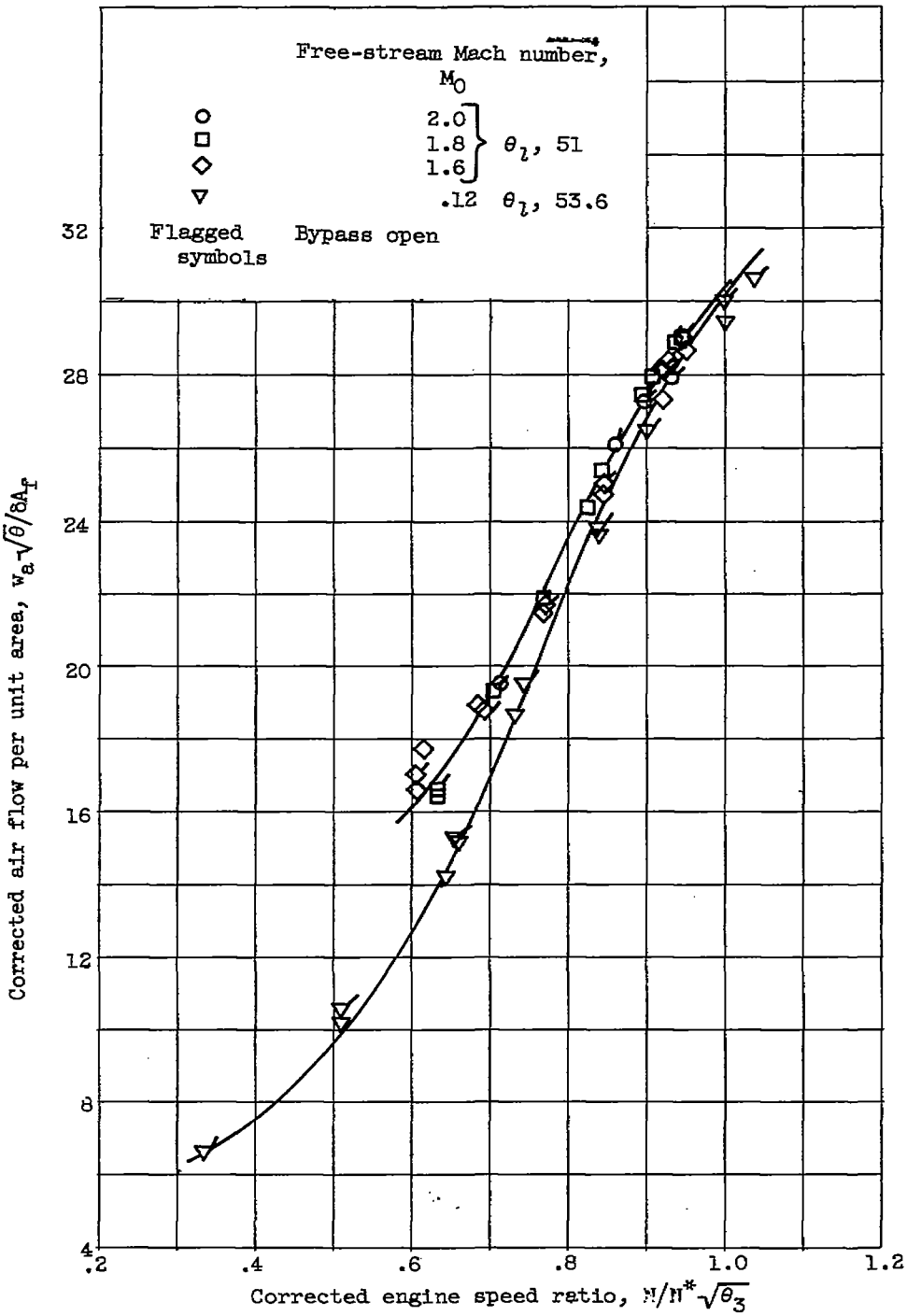

(a) Corrected air flow.

Figure 5. - Generalized engine characteristics.

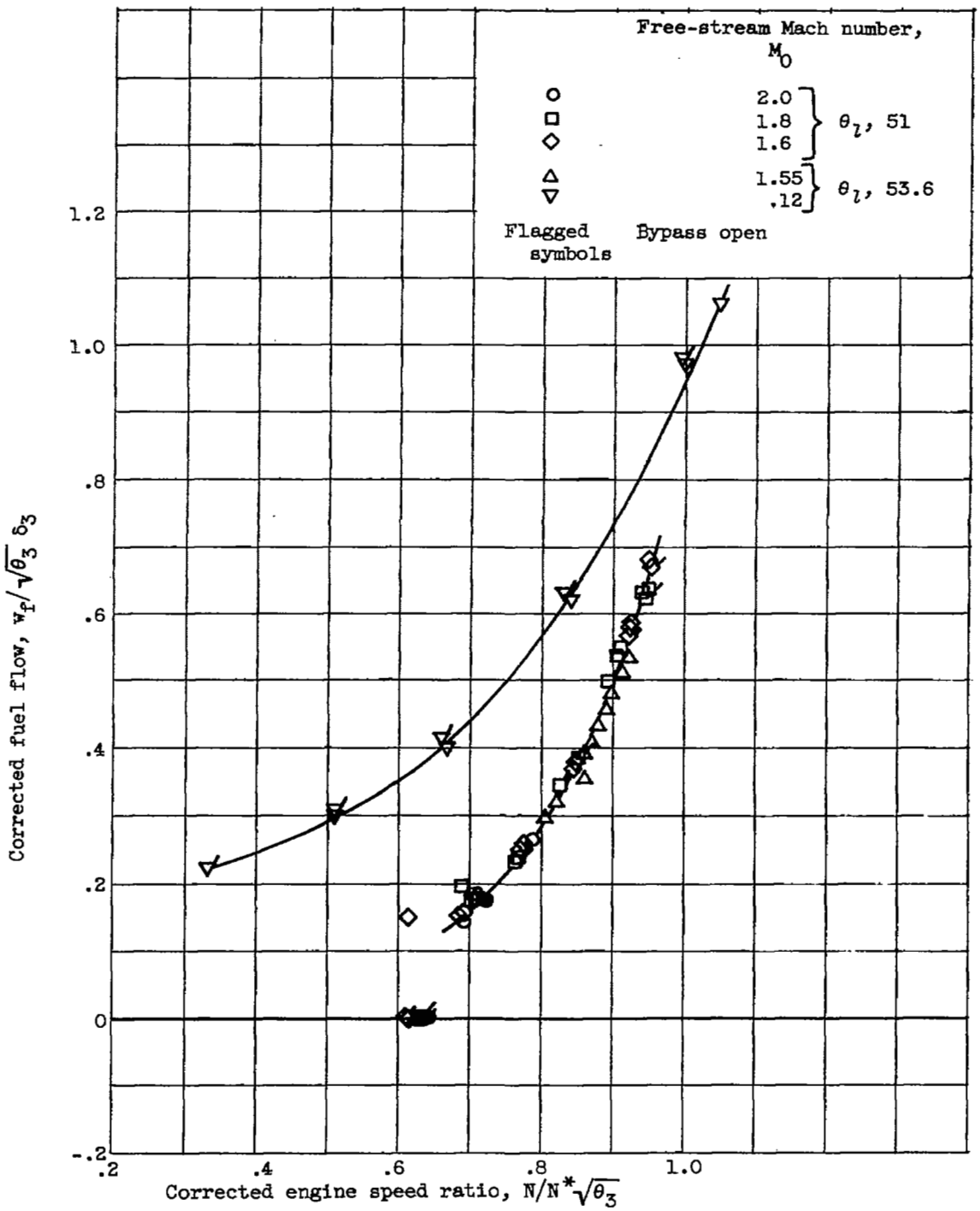

(b) Corrected fuel flow.

Figure 5. - Continued. Generalized engine characteristics.

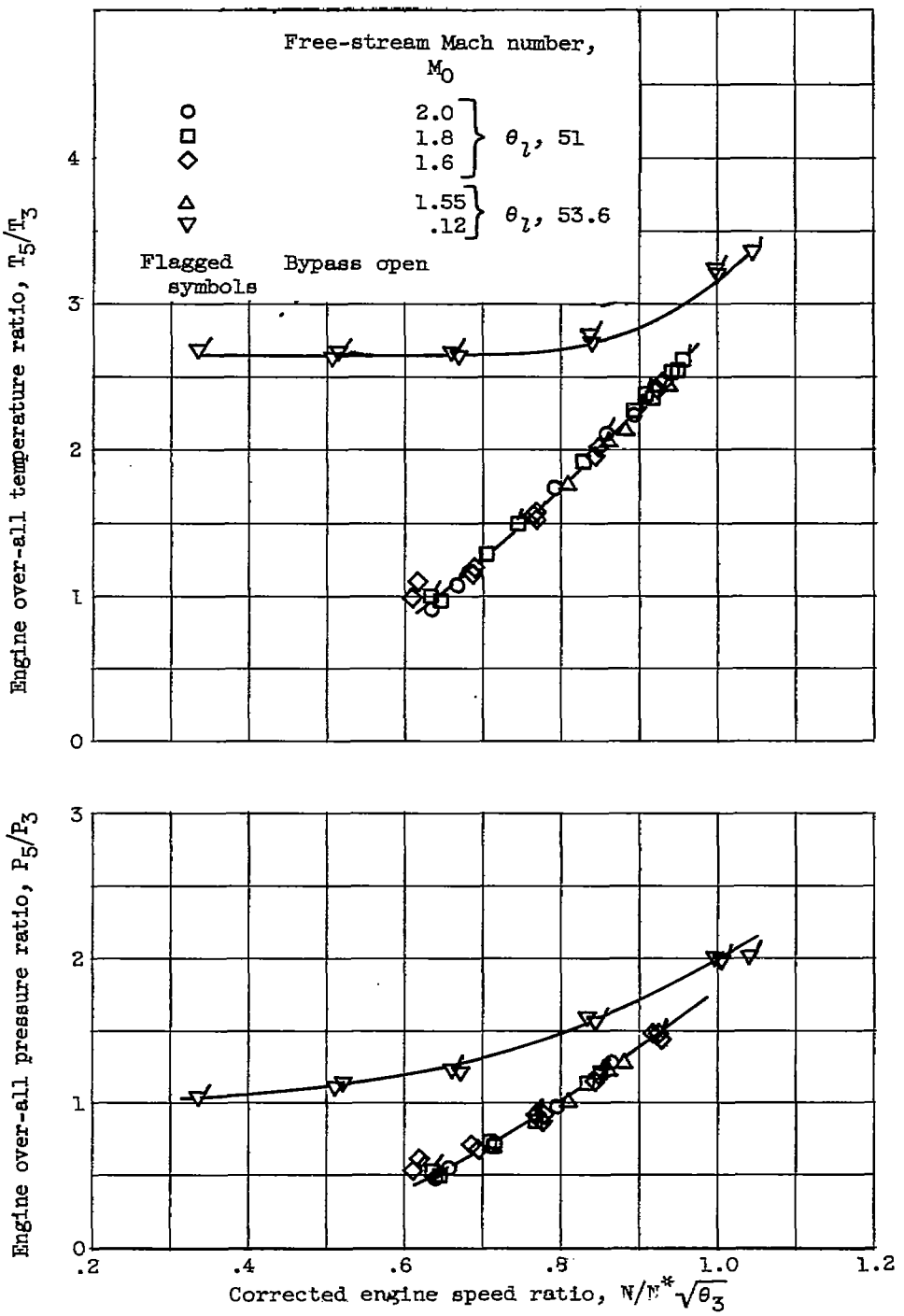

(c) Engine pressure and temperature ratios.

Figure 5. - Continued. Generalized engine characteristics.

[redacted]

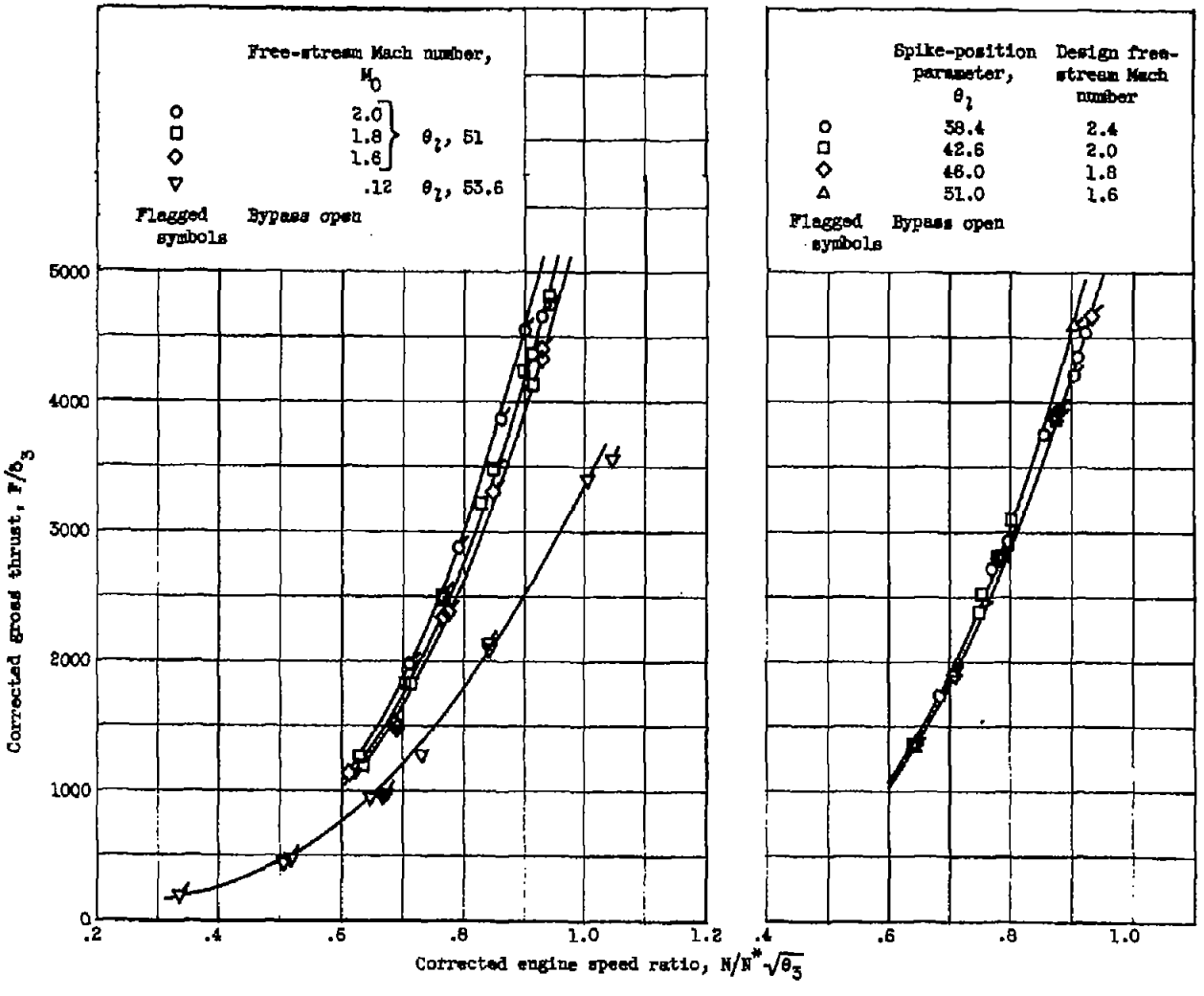

(d) Corrected gross thrust. Spike-position parameter, θ_1, 51 and 53.6.

(e) Corrected gross thrust. Free-stream Mach number, M_0, 2.0.

Figure 5. - Concluded. Generalized engine characteristics.

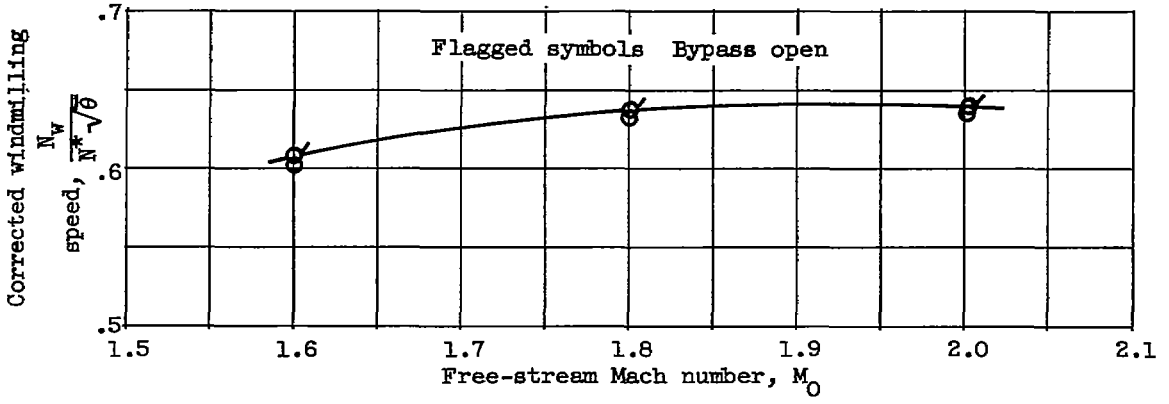

Figure 6. - Variation of engine windmilling speed with free-stream Mach number. Spike-position parameter, 51.

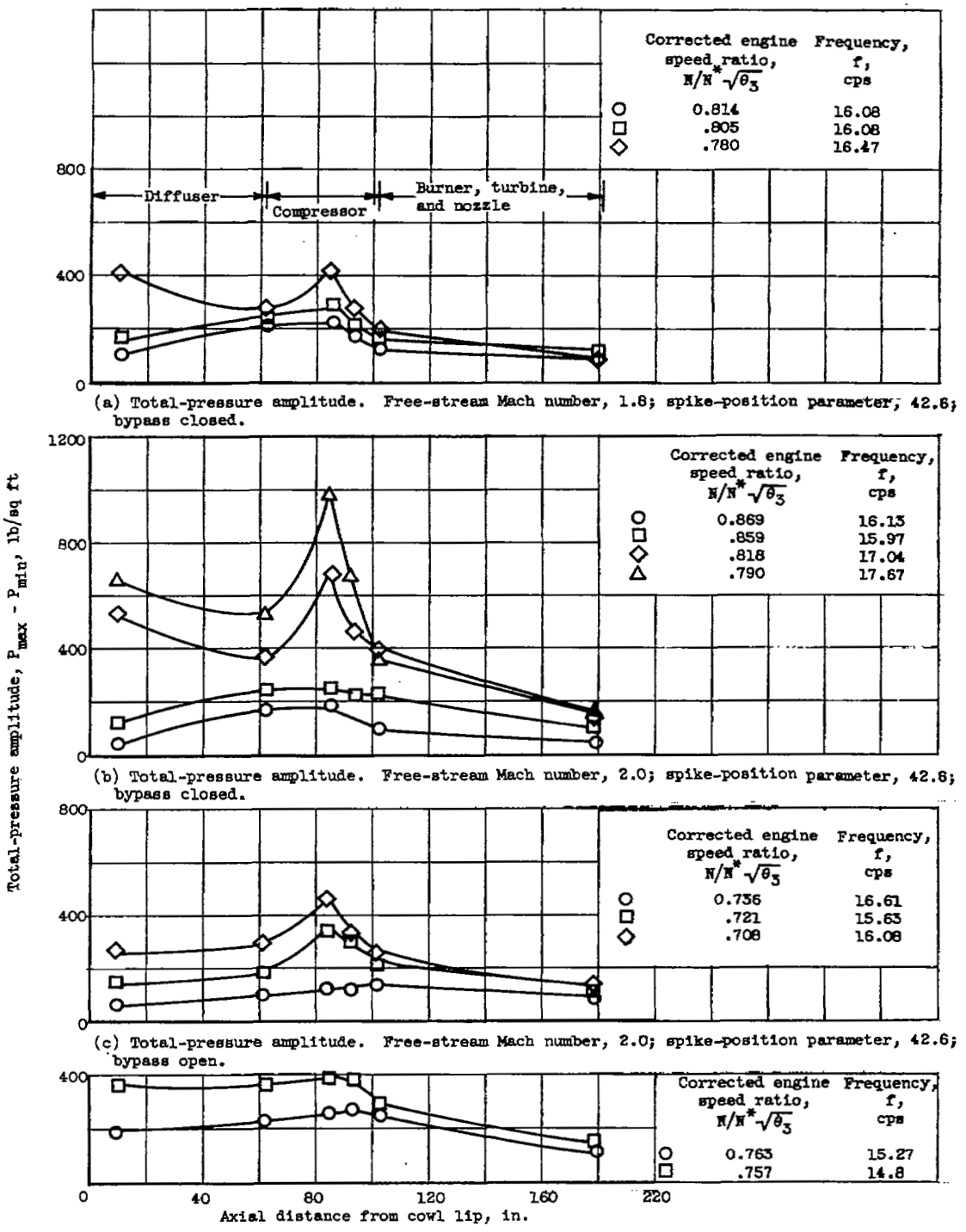

(a) Total-pressure amplitude. Free-stream Mach number, 1.8; spike-position parameter, 42.8; bypass closed.

(b) Total-pressure amplitude. Free-stream Mach number, 2.0; spike-position parameter, 42.8; bypass closed.

(c) Total-pressure amplitude. Free-stream Mach number, 2.0; spike-position parameter, 42.6; bypass open.

(d) Total-pressure amplitude. Free-stream Mach number, 2.0; spike-position parameter, 38.4; bypass closed.

Figure 7. - Pulse propagation through inlet and engine.

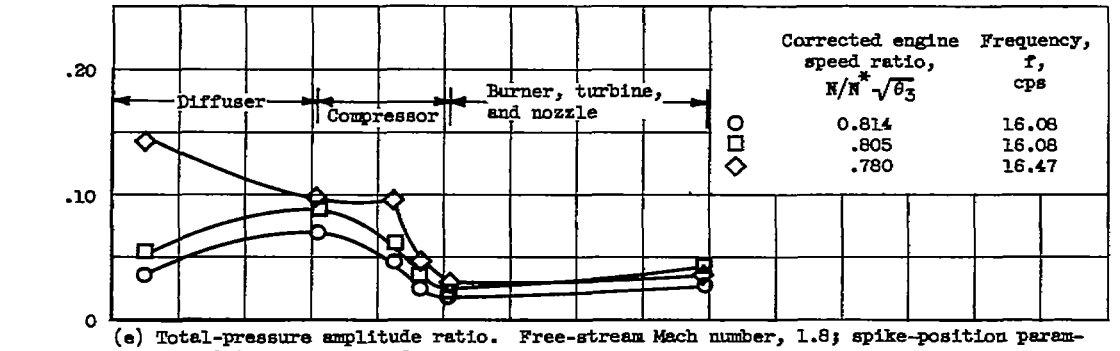

(e) Total-pressure amplitude ratio. Free-stream Mach number, 1.8; spike-position parameter, 42.6; bypass closed.

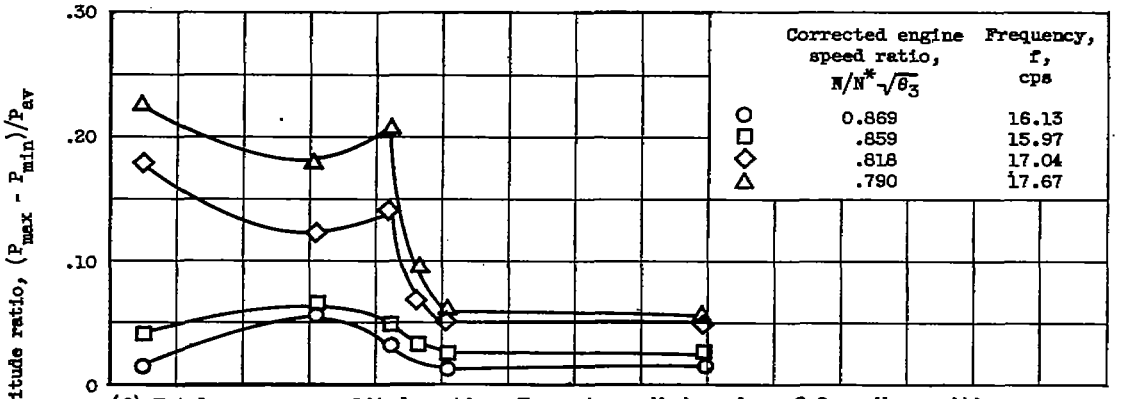

(f) Total-pressure amplitude ratio. Free-stream Mach number, 2.0; spike-position parameter, 42.6; bypass closed.

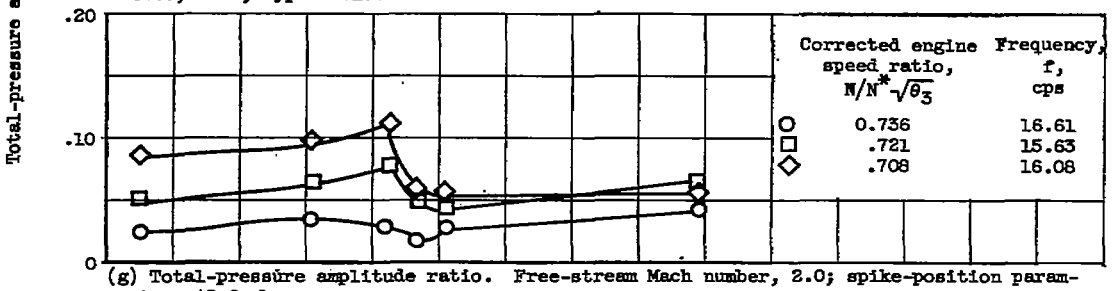

(g) Total-pressure amplitude ratio. Free-stream Mach number, 2.0; spike-position parameter, 42.6; bypass open.

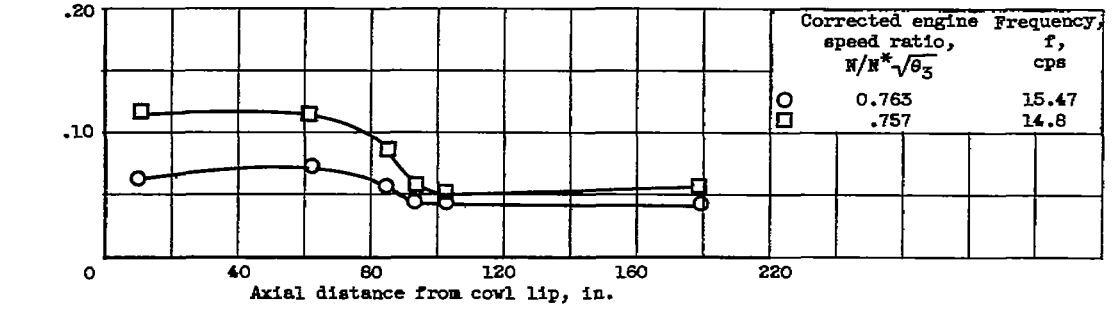

Total-pressure amplitude ratio, $(P_{max} - P_{min})/P_{av}$

(h) Total-pressure amplitude ratio. Free-stream Mach number, 2.0; spike-position parameter, 38.4; bypass closed.

Figure 7. - Concluded. Pulse propagation through inlet and engine.

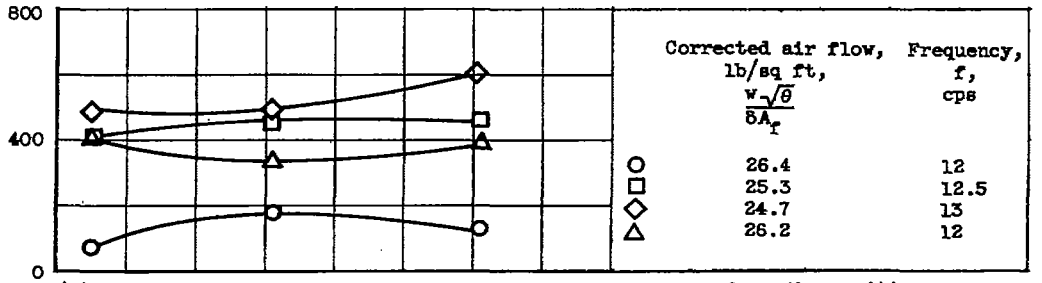

(a) Total-pressure amplitude. Free-stream Mach number, 1.8; spike-position parameter, 42.6; bypass closed.

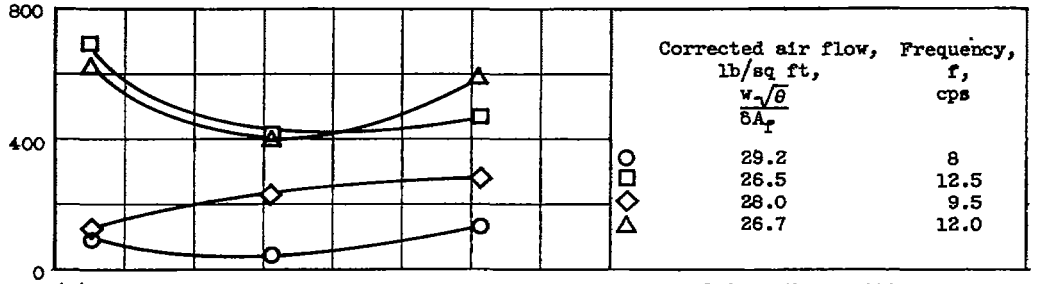

(b) Total-pressure amplitude. Free-stream Mach number, 2.0; spike-position parameter, 42.6; bypass closed.

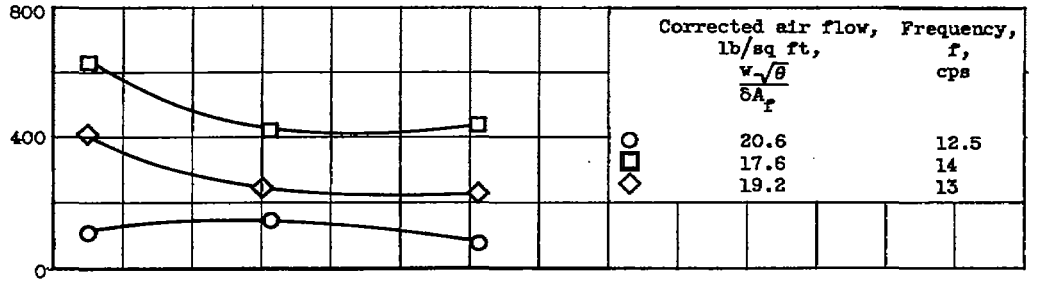

(c) Total-pressure amplitude. Free-stream Mach number, 2.0; spike-position parameter, 42.6; bypass open.

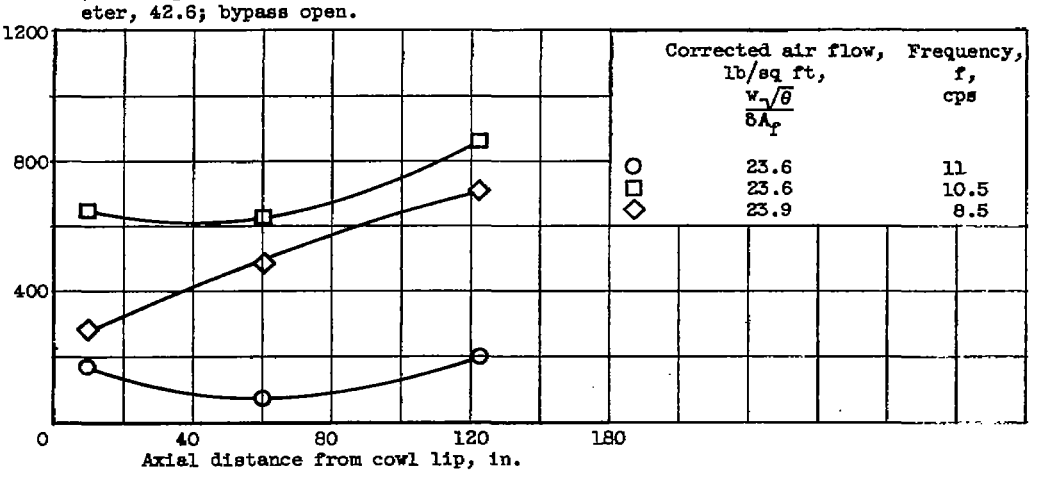

Total-pressure amplitude, $P_{max} - P_{min}$, lb/sq ft

(d) Total-pressure amplitude. Free-stream Mach number, 2.0; spike-position parameter, 38.4; bypass closed.

Figure 8. - Pulse propagation through nacelle. Engine not installed.

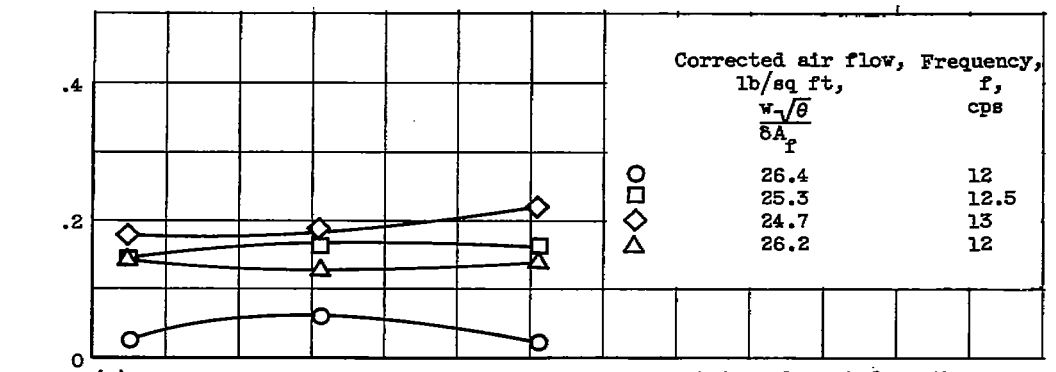

(e) Total-pressure amplitude ratio. Free-stream Mach number, 1.8; spike-position parameter, 42.6; bypass closed.

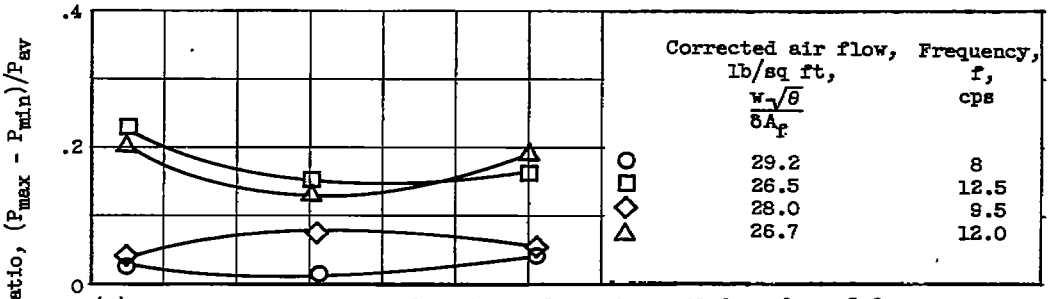

(f) Total-pressure amplitude ratio. Free-stream Mach number, 2.0; spike-position parameter, 42.6; bypass closed.

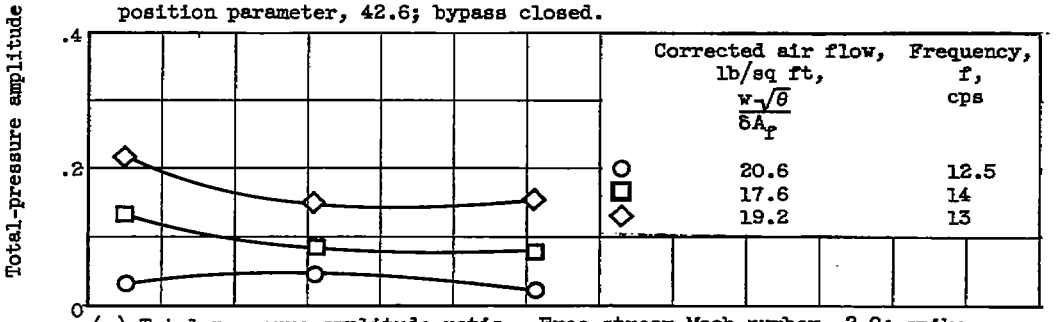

(g) Total-pressure amplitude ratio. Free-stream Mach number, 2.0; spike-position parameter, 42.6; bypass open.

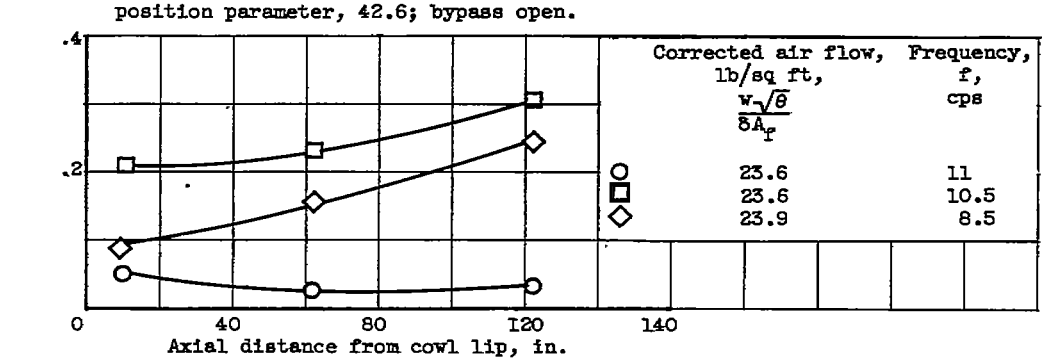

Total-pressure amplitude ratio, $(P_{max} - P_{min})/P_{sv}$

(h) Total-pressure amplitude ratio. Free-stream Mach number, 2.0; spike-position parameter, 38.4; bypass closed.

Figure 8. - Concluded. Pulse propagation through nacelle. Engine not installed.

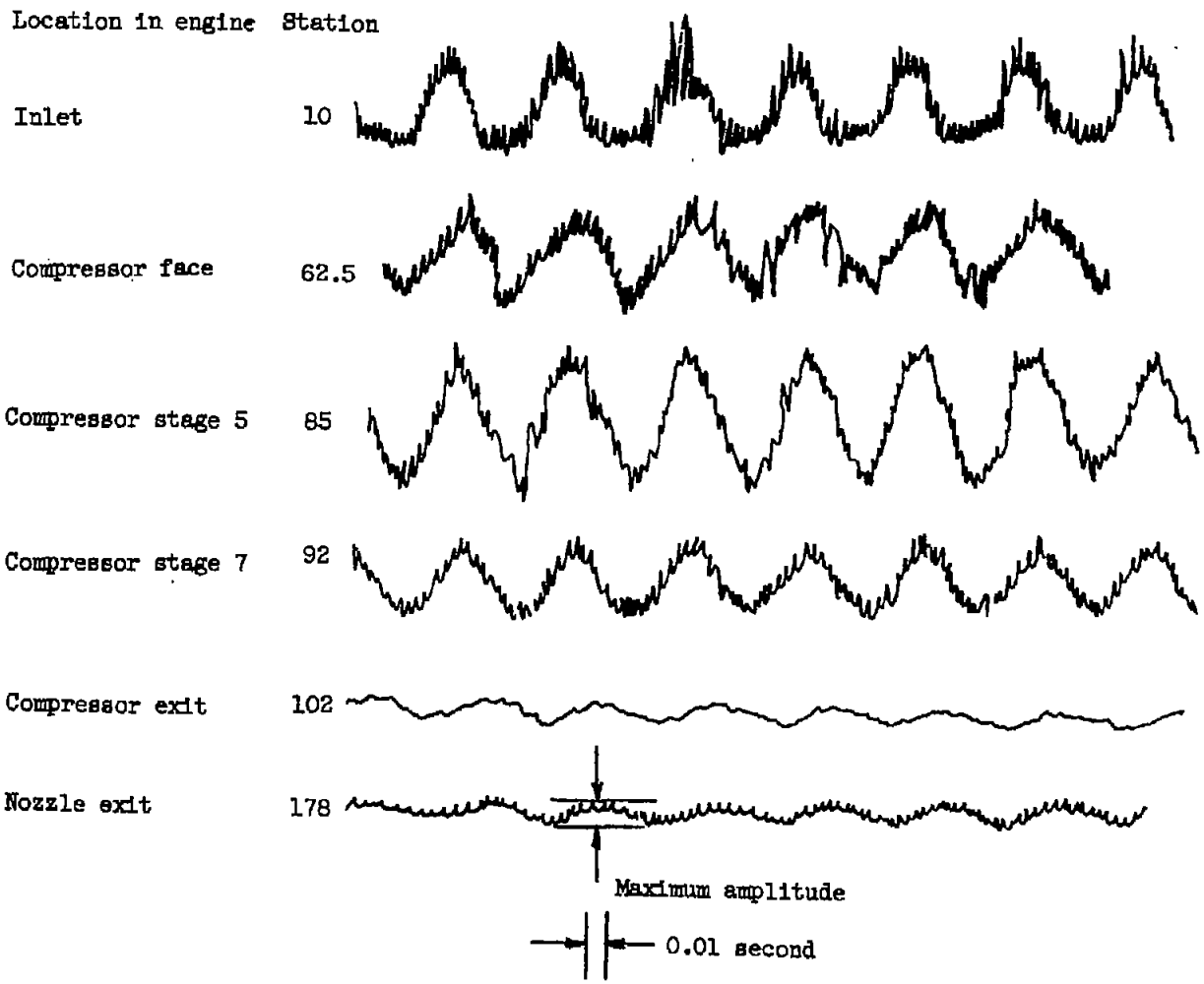

Figure 9. - Typical pulse amplitude traces for stations throughout inlet and engine.

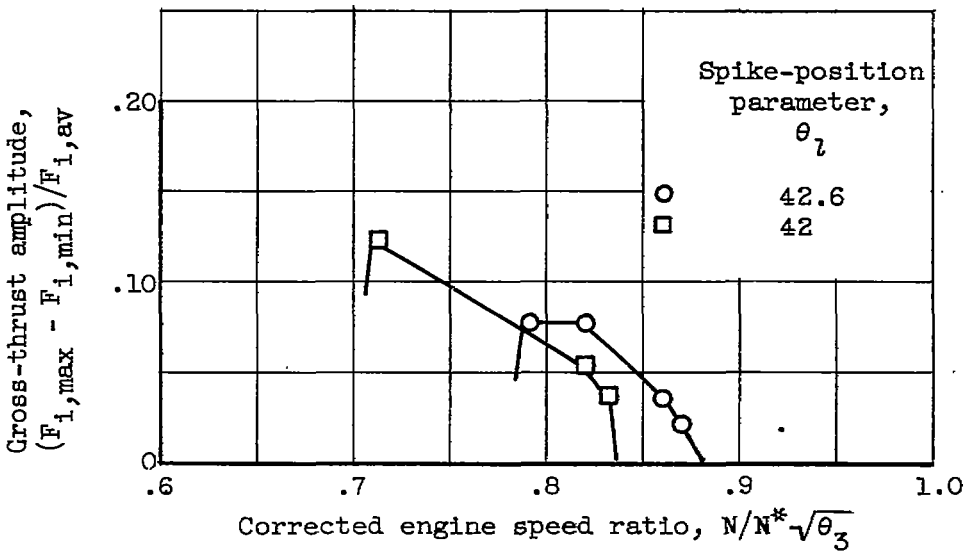

Figure 10. - Effect of inlet pulsing on engine gross thrust. Free-stream Mach number, 2.0; bypass closed.